3D MODELING OF IRAN AND SURROUNDING AREAS FROM SIMULTANEOUS INVERSION OF MULTIPLE GEOPHYSICAL DATASETS

Charles J. Ammon[1] and Monica Maceira[2]

Penn State[1] and Los Alamos National Laboratory[2]

Sponsored by the Air Force Research Laboratory and the National Nuclear Security Administration

Award Nos. FA8718-09C-0007[1] and LA09-BAA09-12-NDD03[2]
Proposal No. BAA09-12

ABSTRACT

The objective of this work is to help improve seismic monitoring technology through the development and application of advanced multivariate inversion techniques to generate realistic, comprehensive, and high-resolution 3D models of the seismic structure of the crust and upper mantle that satisfy independent geophysical datasets. Our focus is on the region surrounding Iran from the east coast of the Mediterranean in the west, to Pakistan in the east, an area of prime importance to nuclear explosion monitoring (NEM), and a region with adequate calibration events to validate our model and to quantify its accuracy. Specifically, we plan to integrate surface-wave dispersion, receiver function, and satellite and ground-based gravity observations to help constrain the shallow seismic structure in the Arabian-Eurasian collision zone. Building on our earlier work combining receiver functions and surface wave dispersion, and surface-wave dispersion and gravity, we plan to continue to integrate geophysical data sets to create more compatible earth models. We also intend to explore geologically based smoothness constraints to help resolve sharp features in the underlying shallow 3D structure.

OBJECTIVES

The National Nuclear Security Administration (NNSA) and Air Force Research Laboratory (AFRL) have decided to investigate 3D modeling as part of the effort to improve knowledge of Earth's compressional and shear velocity structure and to enable a reduction of uncertainty in our ability to accurately detect, locate, and identify small (mb < 4) seismic events, which will lead to improved capabilities for NEM. For seismically active areas, with good ground-truth event coverage, earth models with limited accuracy can be corrected by interpolating results from nearby 'ground-truth' events (using the kriging methodology) making it possible to detect, locate, and identify large events even with limited resolution of Earth's structure. However, such approaches may not be effective for smaller events, and remain a challenge for aseismic regions. To improve monitoring capability in such instances, we must develop better seismic models.

The objective of this work is to help improve seismic monitoring technology through the development and application of advanced multivariate inversion techniques to generate realistic, comprehensive, and high-resolution 3D models of the seismic structure of the crust and upper mantle that satisfy independent geophysical datasets. Our focus is on the region surrounding Iran (Figure 1) from the east coast of the Mediterranean in the west, to Pakistan in the east, an area of prime importance to NEM, and a region with adequate calibration events to validate our models and to quantify their accuracy.

Background

Estimating subsurface geologic variations is a challenge. Seismologists have worked on the problem for more than a century (e.g., Milne, 1899; Macelwane and Sohon, 1936; Dahlen and Tromp, 1999). As data quantity and quality and computational ability have improved, we have made important advances in our understanding of the subsurface. Our best knowledge applies to the shallowest regions as well as depths with the sharpest global interfaces (sediment-basement contacts, the base of the crust, base of the mantle, and transitions near 410 km and 660 km depths), where resolution is improved as a result of the strong interactions of body waves with sharp geologic transitions (e.g., Helmberger, 1968; Langston, 1979; Shearer, 1991; Lay t al., 2004). We have also done well modeling regions with smooth velocity changes such as the lower mantle, which allows us to exploit the information in teleseismic body-wave travel times to locate seismic sources reasonably well (e.g., Kennett and Engdahl, 1991). Still, many details within and just beneath the lithosphere elude us. We have been able to surmise that geologic variations here are substantial, and we know that they frustrate attempts to use robust observations such as regional seismic travel times to locate events in many parts of the Earth (e.g., Bondar et al., 2004).

Travel-time based tomography opened the doors to 3D imaging but the models remain blurry, often suffer from interpretational ambiguity, and are not easily used to predict other, independent seismic observations. From our own analyses (Maceira et al., 2005), we have seen how high-resolution surface-wave tomography fails to produce the extremes in seismic shear-wave speed that are evident from independent observations (we discuss more details below). In particular, achieving a model with low enough seismic wave speeds within the Tarim Basin to match seismograms from high-quality observations remains an issue. Waveform tomography methods improve the situation somewhat, including information from both the amplitude and phase of the signal, but restriction of these methods to lower frequency bands limits the resolution of the methods. More recent finite-frequency methods (e.g., Zhou et al., 2004; Dahlen and Zhou, 2006) and adjoint methods (e.g., Tarantola, 1984; Tromp et al., 2008) offer more complete approaches to modeling waveforms and computing sensitivity kernels. But even these approaches face limits imposed by data bandwidth. In any event, such fully 3D waveform methods could benefit greatly from accurate, if approximate, starting models derived from more piecewise interpretation of seismic observables combined with other observations.

RESEARCH ACCOMPLISHED

Our award was made late in the Spring of 2009, so much of this section is a review of earlier work upon which future work will be based – and much of that work was more thoroughly documented in earlier Seismic and Monitoring Research Review Proceedings. We direct the reader to those compilations for greater detail. We begin with a simple conceptual illustration of the challenges we face.

Including Geologic Information

Geologic boundaries can be sharp, and a sharp geologic transition can cause problems when we use smooth seismic models to predict observations for events or stations located near the sharp geologic transition (throughout this report sharp should be interpreted to mean sharp relative to typical seismic wavelengths). A smooth model can predict the travel times well if the source and the station are located in regions with smooth velocity structures that are well modeled in smooth earth models. Thus to be generally applicable, our models should contain sharp features where needed (ocean-continent transitions, across major geologic terrane boundaries, etc.). How can we reconstruct geologic images with sharp lateral boundaries? Or how can we use long-period observations to create models that we can use to estimate short-period wave travel times and amplitudes? Imaging sharp boundaries requires broadband observations. We are, however, usually limited in the short period bands because of their strong sensitivity to structure and substantial spatial aliasing; we are often limited at the long-period end by noise (i.e., long-period signals from many small events are smaller than background seismic ground motions). Even when they are available, long period signals average the heterogeneity over broad regions. Thus arises the conundrum of resolving geologic detail needed to explain short-period observations using long-period data, which leads to the problems associated with using models derived using long periods to account for or remove propagation effects from short-period signals.

To produce models that have realistic ‘sharp’ boundaries requires that we include independent information on the location of those boundaries. Such information is available (for the shallow part of the model) in independent data sets such as gravity, surface geologic maps, and even something as simple as topography. As part of this work, we plan to resolve sharp features by adapting our imaging algorithms to allow the inclusion of geologic information on the location and nature of the boundary into shear-velocity inversions that permit such features (implemented through custom geologic smoothness constraints that allow velocities to be de-correlated across major geologic transitions). Including a priori information into an inversion is obviously only as good as the information that is included. Thus the inclusion of this type of information into the reconstruction of shear-velocity models of the subsurface must proceed carefully and include documentation of the importance of the assumed a priori information on the resulting model. From a probabilistic approach, uncertainties on the a priori information need to be combined and included in the computations of the shear-wave speeds.

Combining Gravity And Rayleigh-Wave Dispersion Observations

Inversion of surface wave dispersion observations is a standard method for estimating 3D shear velocity structure of Earth’s crust and upper mantle. Nevertheless, it is well known that traditional state-of-the-art inversion techniques suffer from poor resolution and nonuniqueness, especially when a single surface wave mode is used (Huang et al., 2003). This is particularly true at shallow depths where the shorter periods, which are primarily sensitive to upper crustal structures, are difficult to measure, especially in tectonically and geologically complex areas. On the other hand, gravity inversions have the greatest resolving power at shallow depths since gravity anomalies decrease in amplitude and increase in wavelength with increasing depth. Gravity measurements also supply constraints on rock density variations. Thus by combining surface-wave dispersion and gravity observations in a single inversion, we can obtain a self-consistent high-resolution 3D shear-velocity/density model with increased resolution of shallow geologic structures.

As an example, consider a small study of a joint surface-wave/gravity inversion performed for the Tarim Basin in western China, which shows the promise of this approach (Maceira and Ammon, 2009). We used gravity observations extracted from the global gravity model derived from the GRACE satellite mission (Tapley et al., 2005). Specifically, we combined Bouguer gravity anomalies with high-resolution surface-wave slowness tomographic maps (Maceira et al., 2005) that provide group velocity dispersion values in the period range between 8 and 100 s. Figure 2 shows the gravity (bottom left) and dispersion (top left) data for a typical cell in our gridded model together with the fits to these observations resulting from the inversion of only dispersion data (second column from the left), from the inversion of only gravity data (third column from the left), and from the joint inversion of both data (right column). The best fit to the gravity anomalies comes from inverting the gravity data alone, meanwhile that same model is not able to fit the dispersion observations. In the same way, the best fit to the observed dispersion values results from inverting dispersion observations alone, but this model does not predict the gravity observations adequately. The 3D velocity model obtained from the joint inversion fits both data simultaneously and reasonably well.

Figure 3 shows the 3D shear-wave speeds derived from the joint inversion at depths of 2, 6, 10, 14, 28, 46, 55, 75, and 100 km. In general, the model agrees well with the main features observed in previous studies (e.g., Villasenor et al., 2001; Ritzwoller et al., 2002; Liang et al., 2004; Hearn et al., 2004; Sun et al., 2004; Sun and Toksoz, 2006; Huang and Zhao, 2006). At shallow depths, low velocities in the Tarim and Junggar basins dominate the images. This is a predictable result because of the clear presence of low velocities associated with the known major sedimentary basins in the tomographic images at short periods (e.g., Maceira et al., 2005). However, the seismic wave speeds in the model's basins is lower than those obtained without including the gravity in the inversion. We think that this is an improvement of our 3D model since seismic discrimination has proven the need of slower velocities at shorter periods (i.e., shallower layers) in those sedimentary basins (H. J. Patton, see Acknowledgements). Although improved, note that the inversion needs further refinement since the high wavenumber features at depths of 75 and 100 km must be artifacts – none of the data used in the inversion can constrain such features (long-period dispersion and gravity).

To quantify the improvement in the shallow parts of the velocity model, we tested the ability of the 3D model to predict surface-wave arrival times at short periods, which is necessary for performing surface-wave magnitude measurements, which can help reduce the detection threshold for seismic discrimination (Taylor and Patton, 2006). We applied the method described by Maceira (2006) to a set of waveforms from 26 nuclear explosions. The new 3D model is able to better predict the arrival of the surface waves at shorter periods. We found that in 73% of the cases, the 3D model from the joint inversion predicts the surface wave arrival times of short period Rayleigh waves when the dispersion-only inversion model does not. The combination of multiple and complementary geophysical data (surface wave dispersion observations and gravity measurements in this case) in a simultaneous inversion not only offers a simple and elegant compromise between fitting both data sets, but actually improves the geophysical model in a tangible way to more confidently and accurately detect, locate, and identify small seismic events, which can help improve NEM capabilities.

CONCLUSIONS

We have initiated a two-year project to map the subsurface geologic variations using seismic dispersion, gravity, and receiver-function observations. We face significant challenges in our efforts to include effective point constraints on structure (receiver functions) with the spatially continuous surface-wave tomography and gravity observations. Our work complements ongoing work at Los Alamos National Laboratory to integrate body-wave travel times into the same formalism. The basic philosophy is that models that explain more data are better. The ultimate utility of the derived earth models is to provide improved predictive capabilities for routine seismic analyses and to provide adequate starting models for 3D waveform inversion approaches.

ACKNOWLEDGEMENTS

We thank the scientists, engineers, and technicians that have created the seismic recording systems and networks that provide excellent broad-band seismic observations. In particular, we thank the USGS and the IRIS Consortia (NSF) who share information and data with the global community in an effective and efficient manner. We also thank the many international groups involved in collecting and sharing quality seismic observations. We also thank Wessel and Smith (1991), the developers of the Generic Mapping Tools software that we use to create many of the illustrations of our research. Finally, we would like to thank Howard J. Patton for information gleaned from personal communications.

REFERENCES

Bondar, I., S. C. Myers, R. E. Engdahl, and E. A. Bergman (2004). Epicentre accuracy based on seismic network criteria, *Geophys. J. Int.* 156: 483–496.

Dahlen, F. A. and J. Tromp (1999). *Theoretical Global Seismology*. Princeton University Press, Princeton, NJ, 1025 pp.

Dahlen, F.A. and Y. Zhou (2006). Surface-wave group-delay and attunuation kernels, *Geophys. J. Int*. 165: 545–554.

Hearn, T. M., S. Wang, J. F. Ni, Z. Xu, Y. Yu, and X. Zhang (2004). Uppermost mantle velocities beneath China and surrounding regions, *J. Geophys. Res*., 109, B11301, doi:10.1029/2003JB002874.

Helmberger, D. (1968). The crust-mantle transition in the Bering Sea, *Bull. Seism. Soc. Am*. 58: 179–214.

Huang, J. and D. Zhao (2006). High-resolution mantle tomography of China and surrounding regions, *J. Geophys. Res.* 111: doi:10.1029/2005JB004066.

Huang, Z., W. Su, Y. Peng, Y. Zheng, and H. Li (2003). Rayleigh wave tomography of China and adjacent regions, *J. Geophys. Res*. 108: doi:10.1029/2001JB001696.

Kennett, B. L. N., and E. R. Engdahl (1991). Traveltimes for Global Earthquake Location and Phase Identification, *Geophys. J. Int*. 105: 429–465.

Langston, C. A. (1979). Structure under Mount Rainier, Washington, inferred from teleseismic body waves, *J. Geophys. Res.* 84: 4749–4762.

Lay, T., E. J. Garnero, and S. Russell (2004). Lateral variation of the D'' Discontinuity beneath the Cocos Plate, *Geophys. Res. Lett*. 31: L15612, doi:10.1029/2004GL020300.

Liang, C., X. Song, and J. Huang (2004). Tomographic inversion of Pn travel times in China, *J. Geophys. Res*. 109: B11304, doi:10.1029/2003JB002789.

Maceira, M. and C. J. Ammon (2009). Joint Inversion of Surface Wave Velocity and Gravity Observations and its Application to Central Asian Basins Shear Velocity Structure, *J. Geophys. Res.* 114: B02314, doi:10.1029/2007JB005157.

Maceira, M. (2006). *Surface Waves, Earth Structure, and Seismic Discrimination*, Ph.D. thesis, The Pennsylvania State University, State College, PA.

Maceira, M, S. R. Taylor, C. J. Ammon, X. Yang (2005). High-resolution Rayleigh wave slowness tomography of central Asia, *J. Geophys. Res*. 110: doi:10.1029/2004JB003429.

Macelwane, J. B. and F. W. Sohon (1936). *Introduction to Theoretical Seismology, Part I, Geodynamics*. John Wiley and Sons, Inc., New York, 336 pp.

Milne, J. (1899). *Earthquakes and Other Earth Movements* (4th Edition). D. Appleton and Company, New York, 376 pp.

Ritzwoller, M. H., M. P. Barmin, A. Villaseñor, A. L. Levshin, and E. R. Engdahl (2002). Pn and Sn tomography across Eurasia to improve regional seismic event locations, *Tectonophys*. 358: 39–55.

Shearer, P. M. (1991). Constraints on upper mantle dscontinuities from observations of long-period reflected and converted phases, *J. Geophys. Res*. 96: 18147–18182.

Sun, Y. and M. N. Toksoz (2006). Crustal structure of China and surrounding regions from P wave traveltime tomography, *J. Geophys. Res*. 111: doi:10.1029/2005JB003962.

Sun, Y., X. Li, S. Kuleli, F. D. Morgan, and M. N. Toksoz (2004). Adaptive moving window method for 3D P-Velocity tomography and its application in China, *Bull. Seismo. Soc. Am.* 94: 740–746.

Tapley, B., J. Ries, S. Bettadpur, D. Chambers, M. Cheng, F. Condi, B. Gunter, Z. Kang, P. Nagel, R. Pastor, t. Pekker, S. Poole, and F. Wang (2005). GGM02 - An improved Earth gravity field model from GRACE, *J. Geodesy*, DOI 10.1007/s00190-005-0480-z.

Tarantola, A. (1984). Inversion of seismic reflection data in the acoustic approximation, *Geophysics* 49: 1259–1266.

Taylor, S. R. and H. J. Patton (2006). A probability of detection method for reducing short-period m_b - M_s false alarm rates, *Bull. Seism. Soc. Am*. 96: 1078–1090.

Tromp, J., D. Komatisch, and Q. Liu (2008). Spectral-element and adjoint methods in seismology, *Communications in Comp. Physics* 3: 1–32.

Villaseñor, A., M. H. Ritzwoller, A L. Levshin, M. P. Barmin, E. R. Engdahl, W. Spakman, and J. Trampert (2001). Shear velocity structure of central Eurasia from inversion of surface wave velocities, *Phys. Earth Planet. Inter*. 123: 169–184.

Wessel, P., and W. H. F. Smith (1991). Free software helps map and display data, *EOS, Trans. of Am. Geophys. Union,* 72: 441–445.

Zhou, Y. F. A. Dahlen, G. Nolet, and G. Laske (2004). Finite-frequency effects in global surface-wave tomography, *Geophys. J. Int*. 163: 1087–1111.

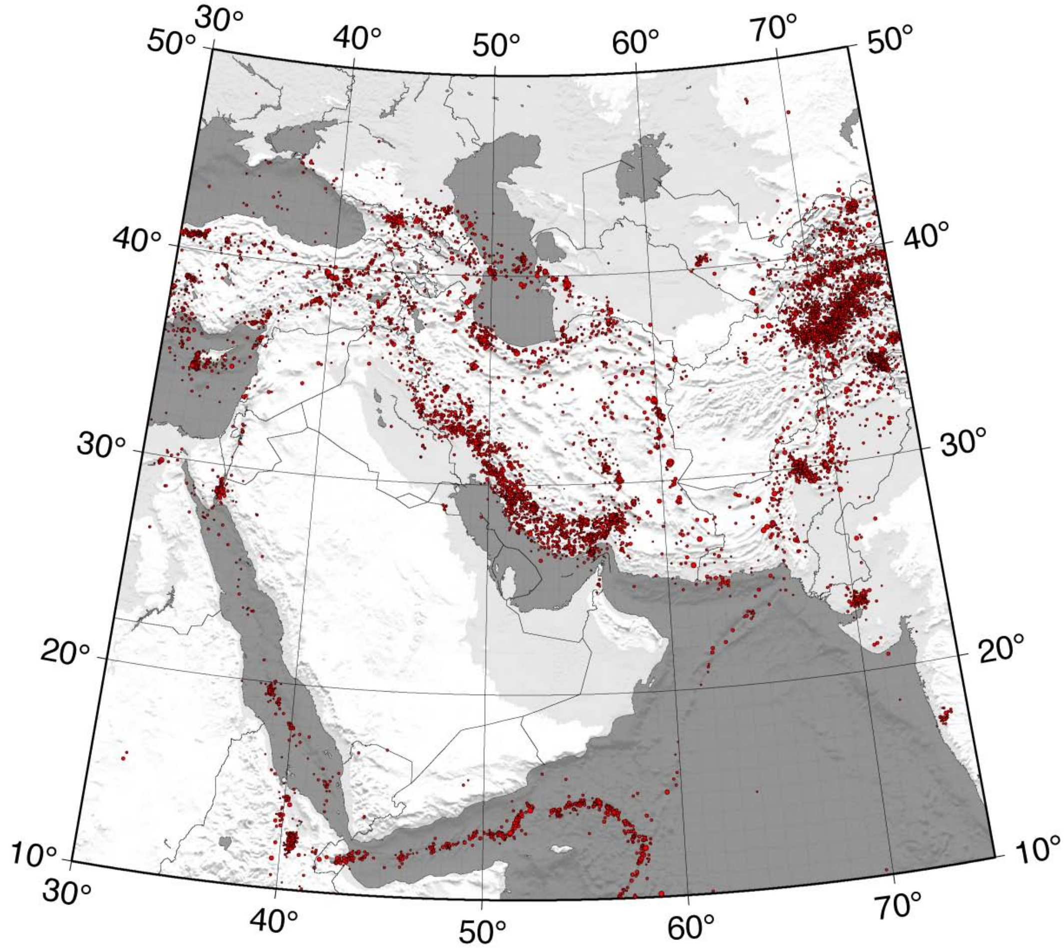

Figure 1. Map of focus region show with topographic and bathymetric shading and moderate to large earthquake locations (magnitudes ≥ 3.5 from 1990 to Spring, 2008). The region contains the Arabian plate and the middle segment of the Alpine to Himalayan collision zone, which is constructed primarily of Phanerozoic terranes amalgamated onto southern Eurasia during the closing of the Tethys Ocean.

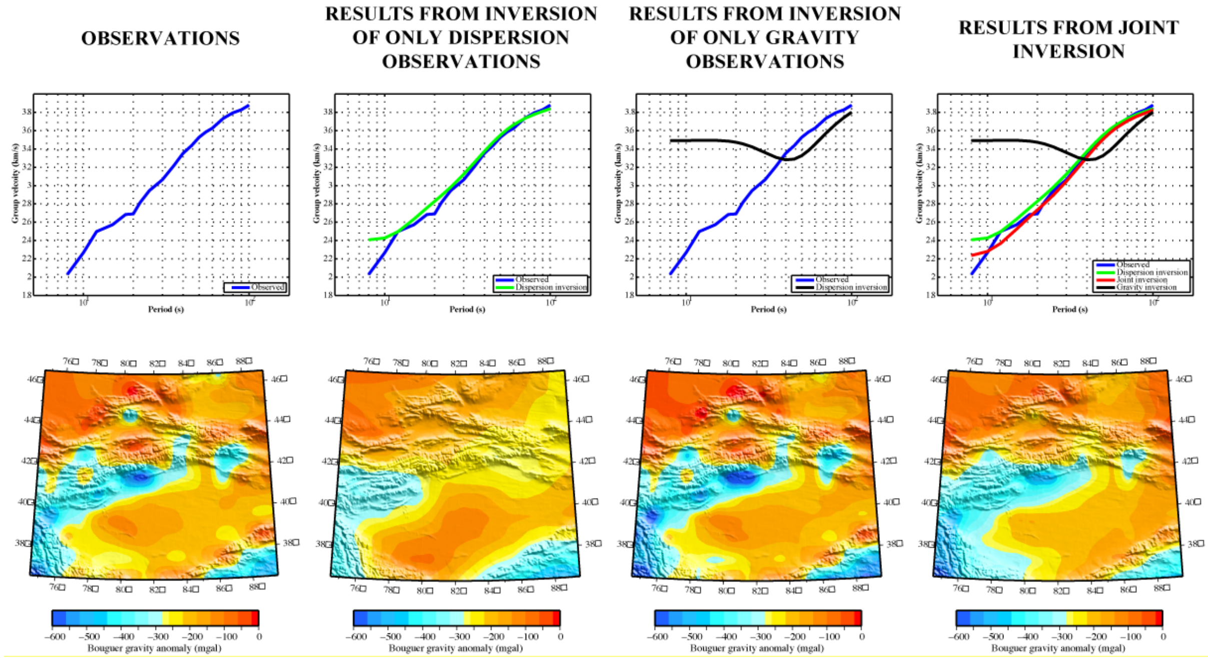

Figure 2. Comparison of data fits from the inversion of only surface wave dispersion observations, the inversion of only gravity observations, and the joint inversion of dispersion and gravity observations. Top panels from left to right: surface wave dispersion data for a typical cell in our gridded model (blue line); fit to the dispersion data from inverting only dispersion data (green line); fit to the dispersion data from inverting only gravity observations (black line); fit to the dispersion data from the joint inversion (red line). Bottom panels from left to right: simple Bouguer anomalies for the region under study; predicted Bouguer anomalies from the model resulting from inverting only dispersion observations; predicted Bouguer anomalies from the model resulting from inverting only gravity observations; predicted Bouguer anomalies from the model resulting from the joint inversion.

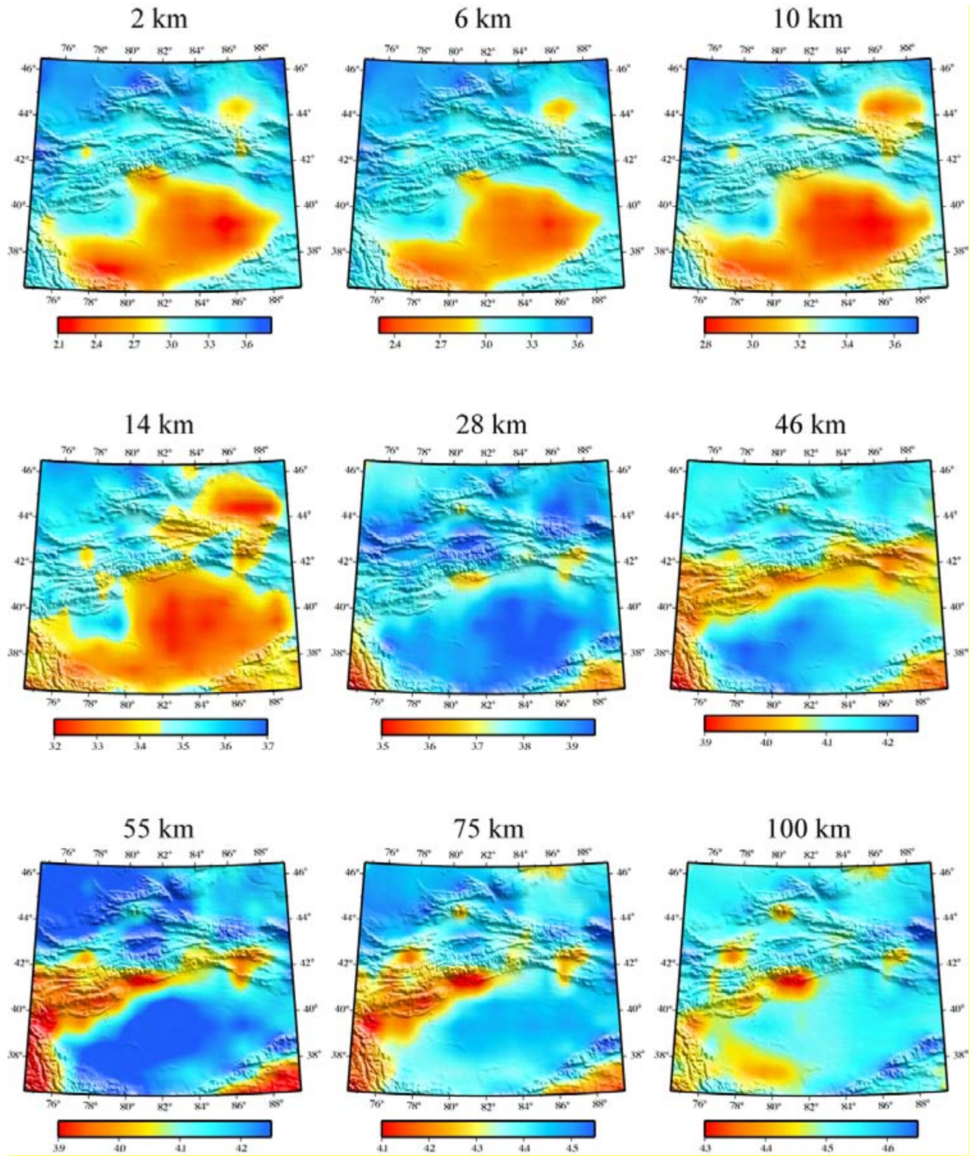

Figure 3. S-wave velocity model at constant depth slices. The depth of each image is shown at the top of each map. Velocity values are expressed in km/s. Note the color scheme is different for each image. The high wavenumber features at depth are clearly artifacts of the simple smoothing scheme used in the current inversion algorithm – none of the data (long-period surface wave dispersion or gravity) can constrain such sharp features at those depths.